Numerical Analysis of Ischemia- and Compression-Induced Injury in Tissue-Engineered Skeletal Muscle Constructs

KARLIEN K. CEELEN, D. GAWLITTA, D. L. BADER, and C. W. J. OOMENS

Department of Biomedical Engineering, Eindhoven University of Technology, P.O. Box 513, Building W-hoog 4.11, 5600 MB Eindhoven, The Netherlands

Abstract—Pressure-related deep tissue injury may develop in skeletal muscle tissue which is subjected to prolonged compression. For early detection, it is important to understand the underlying damage processes. Gawlitta *et al.* [Gawlitta, D., C. W. J. Oomens, D. L. Bader, F. P. T. Baaijens, and C. V. C. Bouten. Temporal differences in the influence of ischemic factors and deformation on the metabolism of engineered skeletal muscle. *J. Appl. Physiol.* 103(2):464–473, 2007b] subjected tissue-engineered muscle constructs to ischemia and deformation to study their effects on viability. Contrary to previous findings, no decrease in viability was found due to compression. However, the nature of their measurement method complicated interpretation of the results, particulary when deformation was involved. Changes in the constructs were assessed by measurements in the surrounding medium. The theoretical model developed in the present study describes metabolism, diffusion, and cell death in the experiments, and accounts for reduced diffusion due to compression. It was demonstrated that the lack of effect of compression on tissue viability, as measured in the experiments, could be explained by the compression-induced decrease in diffusivity. Compression did lead to considerable cell death but this could not be measured by Gawlitta *et al.* [Gawlitta, D., C. W. J. Oomens, D. L. Bader, F. P. T. Baaijens, and C. V. C. Bouten. Temporal differences in the influence of ischemic factors and deformation on the metabolism of engineered skeletal muscle. *J. Appl. Physiol.* 103(2):464–473, 2007b] because diffusion of the cell death marker to the medium was limited. This study shows that a proper description of transport processes is essential for a correct interpretation of experiments in which indirect measurement methods are used.

Keywords—Deformation, Pressure ulcers, Deep tissue injury, Etiology, Damage, Diffusion.

INTRODUCTION

Pressure ulcers may develop when tissue is subjected to prolonged periods of compression. They can start either in the skin from where they may progress towards deeper tissue layers, or in skeletal muscle tissue. The latter type of pressure ulcer is called pressure-related deep tissue injury, which is characterized by an intact layer of skin at its early stages. This makes early detection difficult. If such deep tissue injury progresses, it becomes a deep wound that does not easily heal.

For early detection, it is important to understand damage initiation in skeletal muscle tissue. It is well-known that ischemia adversely affects tissue viability, and it is widely accepted that this is one of the causative factors of pressure ulcers.[7,15] However, there are other factors that may cause damage, such as impaired lymphatic drainage,[18] reperfusion injury[2,12] and cellular deformation.[3,4,9,19] The result is disturbed homeostasis in the tissue, probably involving nutrients, oxygen, waste products, ions, and fluid transport, which may culminate in a pressure ulcer.

Gawlitta *et al.*[10] attempted to unravel the effects of ischemia and/or tissue compression on tissue viability in an *in vitro* set-up. Tissue-engineered murine muscle constructs were subjected to several different conditions associated with ischemia, as well as external compression, both separately and combined. Cell death was indirectly measured by means of the concentration of lactate dehydrogenase (LDH) in the medium, which is released when the cell membrane integrity is compromised. Compression did not lead to increased LDH concentrations, apparently in contradiction with earlier studies that did show cell death due to compression.[3,4,9,20]

Results were however difficult to interpret due to the nature of the adopted method. Changes within the tissue construct were assessed by measurement of concentrations of certain biomolecules within the surrounding medium. This implies that there may be a

Address correspondence to C. W. J. Oomens, Department of Biomedical Engineering, Eindhoven University of Technology, P.O. Box 513, Building W-hoog 4.11, 5600 MB Eindhoven, The Netherlands. Electronic mail: k.k.ceelen@tue.nl, karlienk@gmail.com, c.w.j.oomens@tue.nl

delay before changes in the construct are reflected in the measurements, due to diffusion. Compression may further complicate interpretation of measurements because it will inevitably decrease diffusivity of large molecules such as LDH.[11]

To enable an interpretation of the set of experiments with interacting processes and diffusive properties, which change with deformation, a phenomenological, theoretical model was developed. With this model we have tried to describe diffusion, cell consumption, and production dynamics addressing the following questions: Can compression-induced impaired diffusion of LDH explain the lack of observed effect of compression on tissue viability? Are there any interactions between ischemia and deformation in terms of tissue injury?

METHODS

Experiments

The experiments by Gawlitta *et al.* are described elsewhere.[10] To review briefly, tissue-engineered 3D muscle constructs were created by suspension of approximately 4×10^6 C2C12 murine skeletal myoblasts (ECACC, Salisbury, UK) per milliliter of a collagen/matrigel mixture, which was then molded between two anchoring points in 6-well plates. After 24 h, the growth medium was replaced by differentiation medium to induce the formation of multinucleated myotubes that were aligned between the anchoring points. After a 7–9 day culture period, the tissue-engineered constructs were suitable for subsequent experimentation.

The constructs were subjected to several aspects of ischemia and compression during a period of 5 days without medium refreshment. Impaired nutrient supply during ischemia was represented by glucose deprivation and hypoxia. Glucose deprivation was accelerated by replacement of high-glucose medium (4.5 g/L; 25 mM) with low-glucose medium (1 g/L; 5 mM). Hypoxia was imposed by incubation in an airtight box which was continuously flushed with a 95% N_2 and 5% CO_2 gas mixture.

Another consequence of ischemia is deficient waste product removal, resulting in lactate accumulation. Although a lack of medium refreshment would eventually result in lactate accumulation, the process was accelerated from the start by adding specific amounts of lactic acid to the culture medium to reduce the pH from 7.4 to 6.5, 6.0, and 5.3 at day 0.

Compression was applied via a weight with spacers underneath to ensure an average of $34 \pm 8\%$ reduction in the height of the central part of the construct.

Everyday, a small medium sample was withdrawn to measure glucose, lactate, and lactate dehydrogenase (LDH) concentrations. The latter was used as an indicator of tissue viability because it leaks out of cells when their membrane integrity has been compromised. At the end of the 5-day period, an MTT-assay (3-(4,5-dimethylthiazol-2yl)-2,5 diphenyltetrazolium-bromide) was performed to assess metabolic activity in the muscle construct.

Gawlitta *et al.*[10] performed two sets of experiments. Because each set came from a different batch of cells the properties of the two sets are a little bit different, meaning that each set had its own control group, that was used to estimate material parameters (see section "Parameter Estimation"). The first set comprised a glucose deprivation group, three lactic acidification groups (pH 6.5, 6.0, and 5.3) and three groups where lactic acidification (pH 6.5) was combined with either hypoxia or compression or both. The second set contained one group subjected to hypoxia, one to compression and one group subjected to hypoxia and compression.

Model Geometry

The wells used to culture skeletal muscle constructs had a surface area of approximately 10 cm^2 (radius 17 mm) and contained approximately 2.5 mL medium.[10] The muscle constructs were approximately 2 mm wide, 0.5 mm thick, and 10 mm long. Since the length of the constructs was much larger than their width, a 2D cross section was chosen as model geometry (Fig. 1).

For the deformation experiments, the geometry was changed by reducing the height of the construct by 40%, accompanied by an increase of 40% in width (right panel in Fig. 1). The total area of medium was kept constant. It should also be noted that a 2D model system was required as the weight on top of the muscle construct blocked diffusion in that direction compared to the control situation.

Model Equations

A 2D finite element code for diffusion, consumption, and production was written in Matlab (The Mathworks, Inc.) with the concentrations of glucose (C_{GL}), lactate (C_{LA}), and lactate dehydrogenase (C_{LDH}) as degrees of freedom (see Appendix). Equations (1)–(3) describe the relations that were assumed in the model:

$$\frac{\partial C_{GL}}{\partial t} = D_{GL}\nabla^2 C_{GL} - (\ell_6 - \bar{C}_{LDH})(1 - f_{LA}C_{LA})\frac{V_m C_{GL}}{K_m + C_{GL}} \quad (1)$$

The change in glucose concentration with time (t) depends on diffusion (D_{GL} is the glucose diffusion coefficient) and consumption. For the latter,
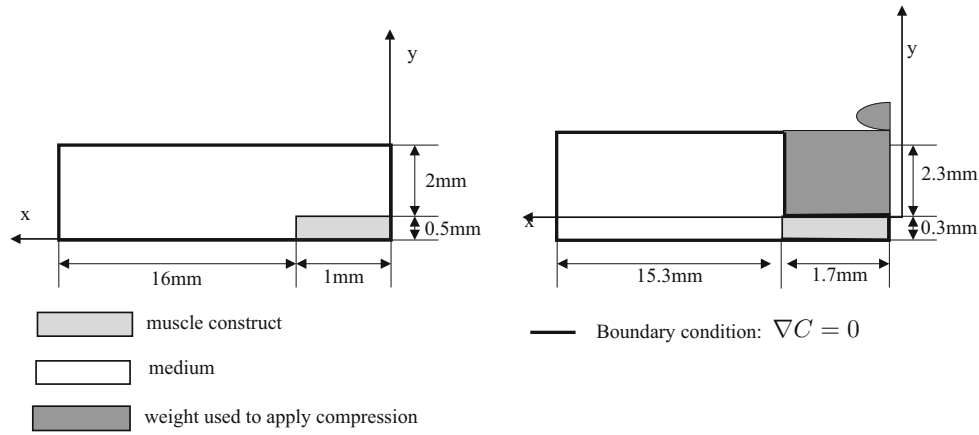
FIGURE 1. Model geometry in the absence (left) and in the presence of compression (right). The *dashed line* is the symmetry line. The *thick solid line* represents the boundary with prescribed no-flow condition.

Michaelis–Menten kinetics were assumed with V_m the maximum glucose consumption rate and K_m the glucose concentration at half maximum consumption rate.

The amount of dead cells was assumed to be directly related to the total amount of LDH that has leaked out of the cells, represented by $\bar{C}_{LDH}$, which is the average LDH concentration in medium and construct at time t. Parameter ℓ_6 is the average LDH concentration when all cells are dead, which is estimated on the basis of the experimental LDH data. Thus the term $\ell_6 - \bar{C}_{LDH}$ accounts for the decrease in the amount of viable cells that consume glucose.

The term $(1 - f_{LA}C_{LA})$ represents the inhibiting effect of lactate accumulation on glucose metabolism, as was observed in the experiments.[10]

The change in lactate concentration with time was modeled with a diffusion term (D_{LA} is the lactate diffusion coefficient) and a production term (second term), namely:

$$\frac{\partial C_{LA}}{\partial t} = D_{LA}\nabla^2 C_{LA}$$
$$+ f_{\frac{LA}{GL}}(\ell_6 - \bar{C}_{LDH})(1 - f_{LA}C_{LA})\frac{V_m C_{GL}}{K_m + C_{GL}} \quad (2)$$

Lactate production is directly coupled to glucose consumption, with factor $f_{\frac{LA}{GL}}$ defining the ratio between these two metabolic processes.

Equation (3) describes the LDH concentration with time, which increases due to LDH leakage from dead cells in the construct:

$$\frac{\partial C_{LDH}}{\partial t} = D_{LDH}\nabla^2 C_{LDH} + \ell_1 + \ell_2\left(\frac{\partial C_{GL}}{\partial t} - \ell_3\right)$$
$$+ \ell_4(C_{LA} - \ell_5). \quad (3)$$

The increase in LDH in control experiments of Gawlitta *et al.*[10] was largely attributed to a basal cell death rate, accounted for by ℓ_1.
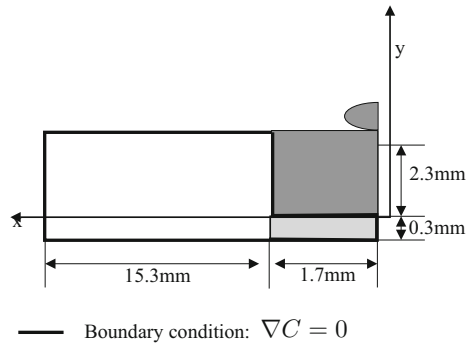
Experiments with high- and low-glucose medium suggested that decreased glucose availability induced LDH release. The equation assumes that viability was determined by the rate of the glucose concentration change as opposed to the absolute concentration. Thus, the term $\ell_2\left(\frac{\partial C_{GL}}{\partial t} - \ell_3\right)$ increased LDH release when the availability of glucose became too low. When glucose availability was still high enough according to the threshold value ℓ_3, this term was set to zero.

Furthermore, the presence of lactate and the accompanying acidification are known to be harmful, as depicted in the term $\ell_4(C_{LA} - \ell_5)$, which accounts for the release of LDH when the local lactate concentration is higher than ℓ_5. For lactate concentrations below ℓ_5, this term was set to zero.

In the above equations, D_{GL}, D_{LA}, and D_{LDH} are the diffusion coefficients of glucose, lactate, and LDH, respectively. The diffusion coefficients in the constructs were estimated based on the Mackie and Meares relation[17]: $D_{construct}/D_{water} = (n_f)^2/(2 - n_f)^2$. With an estimated fluid fraction n_f of 95%, $D_{construct}/D_{water} = 0.82$, which falls within the range Gefen *et al.*[11] measured for diffusion coefficients in tissue-engineered muscle constructs. Compression was assumed to lead to a 50% reduction in D_{LDH}, as has been measured by Gefen *et al.*[11] for molecules of comparable size. Glucose (~180 Da) and lactate (~90 Da) are much smaller than LDH (~140 kDa) and their diffusion was assumed to be unaffected by compression. Table 1 lists the values of the diffusion coefficients used for both the medium and the construct.

Production and consumption terms are only appropriate in the construct, while in the medium only the diffusion term is employed. Natural boundary conditions were imposed on all outer boundaries to describe that they were impenetrable:

$$\nabla C_{LDH} = \nabla C_{LA} = \nabla C_{GLA} = 0.$$

The flux was also zero across the symmetry-axis. In Fig. 1 the boundaries with prescribed zero flux are depicted with a thick solid line. Day 0 concentrations from Gawlitta *et al.*[10] were applied as initial conditions. The day 0 concentration for glucose was taken the same in the muscle as in the medium. Based on the diffusion constant for glucose we would expect that the muscle is in equilibrium with the medium in 40 min to 1 h. For LDH and lactate the initial concentrations are zero, except in the simulations that started with lower pH-value (number 3, 4, 5, 6, 7, and 8). In these cases the initial lactate concentrations in medium and skeletal muscle were based on the experimental starting values (see Fig. 4).

For a comparison between simulated and experimental medium concentrations, the simulated concentrations in the medium were spatially averaged to obtain a representative value.

Parameter Estimation

Muscle constructs that are engineered from different batches of cells will in general not lead to the same parameter set. Unfortunately not all experiments could be performed with one batch, so it was necessary to use two parameter sets for two experimental groups based on different batches. That is why two sets of control experiments were performed with high glucose medium. From the glucose as a function of time curve V_m and K_m are estimated. The LDH vs. time curve for the control determines ℓ_1 and ℓ_6. The ℓ_2 and ℓ_3 values based on the low glucose curve were used in both sets. The parameters ℓ_4, ℓ_5, and f_{LA} are derived from the experiments with different starting values for the pH. The latter parameters were estimated on the glucose concentrations at day 5. Because pH and lactate concentrations were measured, both the ratio between LA production and GL consumption $f_{\frac{LA}{GL}}$ was known for each experiment. To summarize, the experiments of control, glucose deprivation, hypoxia, different pH were used for parameter estimation. Only the experiments of combined effects of ischemia and compression were used for model prediction.

RESULTS

The results from both experimental sets that involved the effect of ischemia alone, were used to find a set of parameters that fitted all situations. However, there were large differences between the control groups of the two data sets for each of the metabolite concentrations, as illustrated in Fig. 2. Thus, two different parameter sets were identified and subsequently used to analyze the experiments which examined the combined effects of ischemia and compression. Table 2 gives an overview of the experimental groups in the following paragraphs.

Separate Effects of Glucose Deprivation and Lactic Acidification

First, the experimental groups from set 1 that examined the effects of either glucose deprivation or lactic acidification were fitted. They were used to find a set of parameters (Table 3) that could subsequently be used to examine the combined effects of lactic acidification with deformation, hypoxia or both (section "Combined Effects of Deformation and Hypoxia with Lactic Acidification").

TABLE 1. Diffusion coefficients.

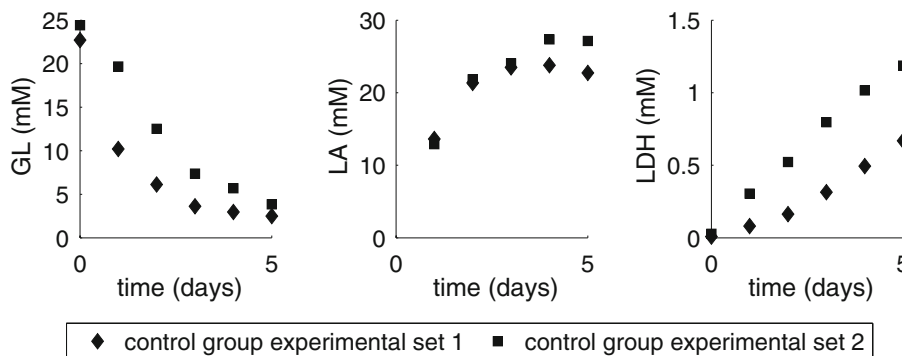|	D_{medium} (10^{-4} mm²/s)	$D_{construct}$ (10^{-4} mm²/s)	
		No compression	Compression
GL	9.0[1]	7.4	7.4
LA	14[13]	11	11
LDH	0.4[11]	0.33	0.16

FIGURE 2. Glucose (GL), lactate (LA), and LDH concentrations with time for control groups from experimental sets 1 and 2. Experiments 1 and 9 (Table 1).

TABLE 2. Overview of experiments.

Number	Experim. group	Section	Deform %	Oxygen %	In. pH	In. Gluc. (g/L)
1	Control 1	3.1, 3.3	0	20	7.4	4.5
2	Low glucose	3.1	0	20	7.4	1
3	pH 6.5	3.1	0	20	6.5	4.5
4	pH 6.0	3.1	0	20	6.0	4.5
5	pH 5.3	3.1	0	20	5.3	4.5
6	pH 6.5 def	3.3	34	20	6.5	4.5
7	pH 6.5 hyp	3.3	0	<6	6.5	4.5
8	pH 6.5 def + hyp	3.3	34	<6	6.5	4.5
9	Control 2	3.2	0	20	7.4	4.5
10	def	3.2	34	20	7.4	4.5
11	hyp	3.2	0	<6	7.4	4.5
12	def + hyp	3.2	34	<6	7.4	4.5

Set 1 comprises experiments 1–8. Set 2 comprises experiments 9–12.

TABLE 3. Parameter sets.

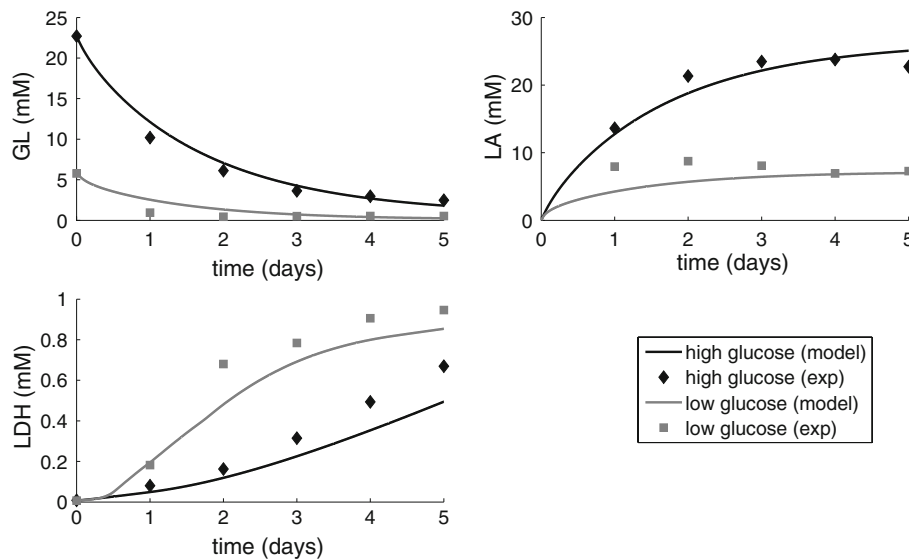| Parameter	Set 1 norm	Set 1 hyp	Set 2 norm	Set 2 hyp
ℓ_1 (mM/day)	4	4	10	10
ℓ_2 (–)	1.0×10^3	1.0×10^3	2.5×10^3	2.5×10^3
ℓ_3 (mM/day)	-6.5×10^{-2}	-6.5×10^{-2}	-6.5×10^{-2}	-6.5×10^{-2}
ℓ_4 (/day)	1.5	1.5	4.25	4.25
ℓ_5 (mM)	20	20	20	20
ℓ_6 (mM)	0.90	0.90	1.40	1.40
V_m (mM/day)	3.0×10^3	3.0×10^3	2.0×10^3	2.0×10^3
K_m (mM)	0.50	0.50	0.50	0.50
f_{LA} (/mM)	0.36	0.26	0.36	0.26
$f_{\frac{LA}{GL}}$ (/mM)	1.2	1.6	1.2	1.6

FIGURE 3. Glucose (GL), lactate (LA), and LDH concentrations with time for control (high glucose) and glucose deprivation experiments (low glucose). Fitting these numerical simulations to the experimental data resulted in parameter set 1. Experiments 1 and 2 (Table 1).

Figure 3 shows the numerical fit to the glucose deprivation (low glucose) and control experiments (high glucose). The glucose and lactate concentrations are described well by the model, although it under-estimates the lactate concentrations at days 1–3 of the low-glucose experiment.

The third panel in Fig. 3 shows the experimental and numerical LDH concentrations. In the control
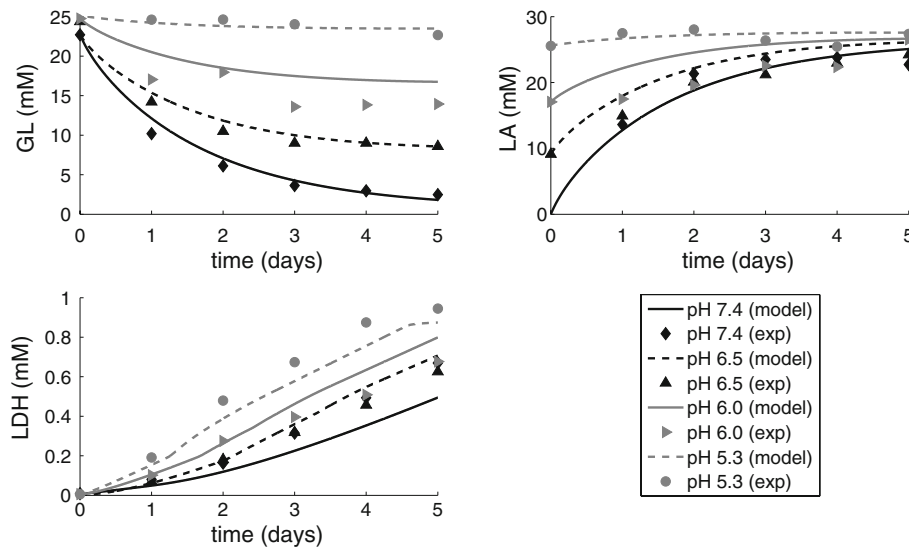
FIGURE 4. Glucose (GL), lactate (LA), and LDH concentrations with time for control (pH 7.4) and lactic acidification experiments (pH 6.5, pH 6.0, and pH 5.3). Fitting these numerical simulations to the experimental data resulted in parameter set 1. Experiments 3, 4, and 5 (Table 1).

group, LDH increased both due to the basal cell death rate and due to lactate accumulation, which explains the nonlinear nature of the curve. The sharp increase in LDH in the low-glucose group is caused by the low glucose availability, as reflected in the ℓ_3-value. Thereafter, it approaches a threshold value as defined by ℓ_6.

The experimental and numerical results for the lactic acidification groups are shown in Fig. 4. The model fits the experimental glucose and lactate concentrations well, except for a small over-prediction of the experimental values at pH 6.0. Despite clearly different rates of glucose consumption and lactate accumulation, the experimental LDH values were only significantly increased compared to the control experiment in the experiment with the lowest pH. In the model, these different lactate accumulations exceed the threshold of ℓ_5 and according to the term $\ell_4(C_{LA} - \ell_5)$ of Eq. (3) this leads to differences in medium LDH concentrations for the different groups. These differences are supported by the MTT measurements from Gawlitta et al.[10] at day 5, which show a monotonic decrease in metabolic activity with decreasing pH.

Separate and Combined Effects of Deformation and Hypoxia

In the second set of experiments, Gawlitta et al.[10] examined the effects of hypoxia and deformation, both separately and combined. The control group in this set yielded LDH concentrations with time which were significantly higher than the corresponding controls from set 1 (Fig. 2). A modified set of model parameters was required (Table 3). In particular, the maximum LDH concentration (ℓ_6) was increased from 0.9 to 1.4 mM and V_m was decreased from 3000 to 2000 mM/day. This implies that the total maximum glucose consumption rate (second term on the right-hand-side of Eq. 1) remained approximately equal. In addition, the parameters that specify the rate of LDH production were multiplied by 2.5 ($\ell_1 = 10$ mM/day, $\ell_2 = -2.5 \times 10^3$, $\ell_4 = 4.25$/day).

Simulation of the hypoxia experiments required some additional parameter changes. The parameter specifying the ratio between lactate production and glucose consumption ($f_{\frac{LA}{GL}}$) was increased from 1.2 to 1.6/mM. The influence of lactate on glucose consumption, as denoted by f_{LA}, was also changed (from 0.36 to 0.26/mM). See Table 3.

Figure 5 shows that the hypoxia experiment was then predicted reasonably well (gray stars and gray solid lines), with an increased lactate production leading to an increased LDH release. However, the model under-predicted lactate concentrations for the deformation experiments (dashed lines). Associated with this, the model over-estimated the glucose concentrations for the combined deformation and hypoxia situation compared to the experimental data.

It is also clear from Fig. 5 that the model underestimated the LDH concentrations in the medium in the deformation experiments (dashed lines). The simulations showed that deformation led to a significant accumulation of LDH in the construct, reaching values in excess of 20 mM after 3 days compared to values below 10 mM in the control experiment. The deviation between the predicted and observed medium
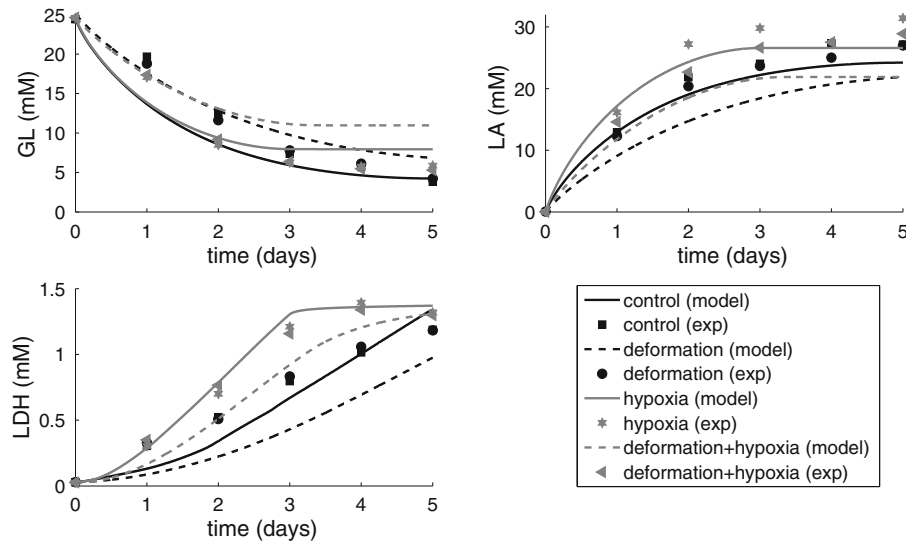
FIGURE 5. Glucose (GL), lactate (LA), and LDH concentrations with time for control, deformation, hypoxia, and combined deformation and hypoxia experiments. Fitting these numerical simulations to the experimental data (with the exception of the experiments in the presence of deformation) resulted in parameter set 2. Experiments 9, 10, 11, and 12 (Table 1).

LDH concentrations had to be caused by deformation-induced LDH leakage, which had not been implemented in Eq. (3).

Based on experiments that were primarily concerned with the effect of deformation on tissue damage,[9] it was assumed that compression demonstrated its effect on tissue viability within the first day. To accommodate this short-term effect in the present model, a constant LDH production was added to Eq. (3). Multiplication of the basal cell death rate by a factor 4 during day 1 (ℓ_1 was increased from 10 to 40 mM/day), raised the LDH concentrations approximately to the experimental values (solid lines in Fig. 6).

Combined Effects of Deformation and Hypoxia with Lactic Acidification

The effects of deformation and hypoxia were also examined in combination with lactic acidification (pH 6.5). These experiments belonged to experimental set 1, hence for the first simulations the parameters were prescribed as in Table 3.

In the experiments presented in Fig. 7, there were no large differences in glucose and lactate concentrations of the different experimental conditions. The predicted values are close to the experimental values, but the glucose predictions are higher in the presence than in the absence of deformation. Correspondingly, the predictions for the lactate concentrations are lower in the presence than in the absence of deformation.

Similar to what was found in the previous paragraph (Fig. 5), the model underestimated the LDH concentrations in the experiments where deformation was involved. Again, the effect of increasing ℓ_1 to four
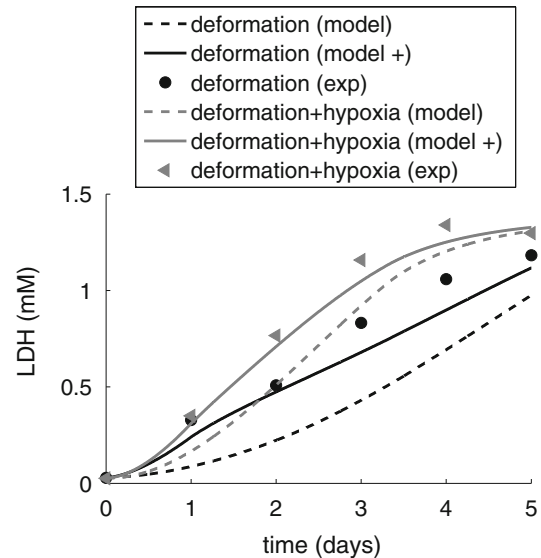

FIGURE 6. LDH concentrations with time for deformation and combined deformation and hypoxia experiments. Experiments 9, 10, 11, and 12 (parameter set 2 (Table 1) was used for the numerical simulations). The dashed model curves are the same as in Fig. 5, i.e., without deformation-induced LDH leakage, and the solid 'model +' curves refer to simulations that included damage due to deformation ($\ell_1 = 40$ mM/day during day 1).

times its initial value during the first day ($\ell_1 = 16$ mM/day) improved the agreement between the model predictions and experimental measurements for the deformation experiments (Fig. 8). This deformation-induced LDH leakage is in agreement with the experimental MTT data,[10] which demonstrated a decreased viability for the experiments in the presence of deformation compared to the control experiment.
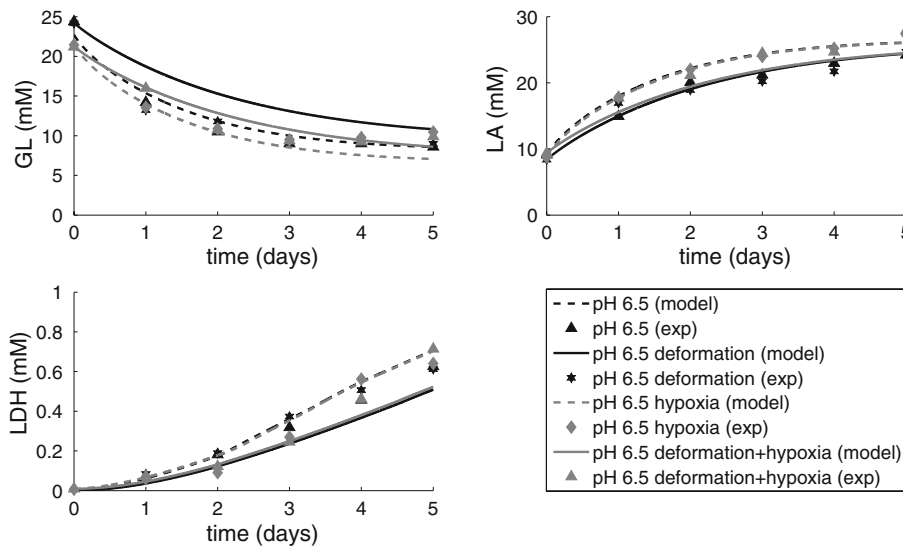
FIGURE 7. Glucose (GL), lactate (LA), and LDH concentrations with time for deformation, hypoxia, and combined deformation and hypoxia experiments at pH 6.5. Experiments 6, 7, and 8 (parameter set 1 (Table 1) was used for the numerical simulations).
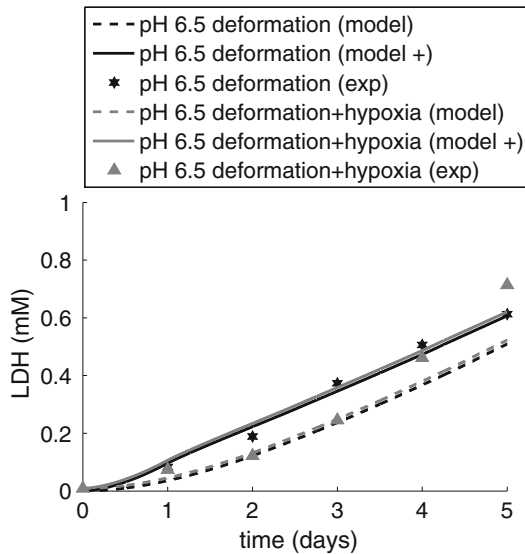

FIGURE 8. LDH concentrations with time for deformation and combined deformation and hypoxia experiments at pH 6.5. Experiments 7 and 8 (parameter set 1 (Table 1) was used for the numerical simulations). The dashed curves are the same as the solid curves in Fig. 7, i.e., without deformation-induced LDH leakage, and the solid 'model +' curves refer to simulations that included damage due to deformation (ℓ_1 = 16 mM/day during day 1).

DISCUSSION

Gawlitta et al.[10] assessed the effects of ischemia and deformation on skeletal muscle constructs by measuring concentrations of selected biomolecules in the medium surrounding the constructs. This implies that molecules have to diffuse from the construct to the medium before they can be measured, which complicates interpretation of the results.

In the present study, a finite element model was developed that described cell consumption and production dynamics and diffusion in a 2D cross section of the experimental set-up. Relatively simple relationships, that could be derived from the experimental results of Gawlitta et al.,[10] were used in the present work to describe muscle cell consumption and production dynamics. This enabled the evaluation of both spatial and temporal profiles of metabolites and a cell death marker.

Deformation was imposed by changing the geometry of the 2D cross section. Combined with the deformation-induced decrease in the LDH diffusion coefficient, this influenced the concentrations of the selected biomolecules. Thus, the effect of deformation on the measurements could be assessed. To be able to find a more local relationship between deformation and damage, a mechanical analysis should be included.[6]

It should be clear that the phenomenological model that was used in this study does not provide an accurate model of muscle metabolism. This would require a much more complex description.[5,8,14,16] The model provides information about glucose consumption and lactate production and the consequences of glucose shortage and lactate concentrations on cell death. It also elucidates aspects of the individual roles of deformation and ischemia on cell death. There are no principle restrictions to extending the more complex descriptions of metabolic processes with a spatial component, but it was beyond the scope of the present paper to include that here.

Gawlitta et al.[10] also measured the pH in their experiments, but this was not included in the present

modeling. The major determinant for the pH in the medium is the lactate concentration. However, the medium is buffered by means of the CO_2 concentration in the incubator (5%) and there may be other acids in the medium in addition to lactate. This makes a theoretical, quantitative description of the pH rather difficult. It would require knowledge on the concentration of those other ions and possibly also how these concentrations are influenced by cell metabolism. Possible effects of a change in pH on glucose consumption or cell death reasons other than lactate concentration changes are thus not described by the model. Qualitatively the pH follows the lactate concentration, so it probably is the dominating factor for pH, but a quantitative prediction is currently not possible.

It should be stressed that the purpose of the present study was to develop and use a model for explaining the experimental results from Gawlitta *et al.*,[10] instead of identifying accurate values for muscle metabolism and damage parameters. Parameters were identified by fitting the model to the experimental groups in which only one aspect of ischemia was imposed. Two parameter sets were required to accommodate the differences between the control groups in the two sets of experiments. The main difference between the two parameter sets was a scaling factor for the parameters specifying the rate of LDH release. With such, it was possible to predict the solute concentrations in the different experimental situations with reasonable accuracy. The model thus proved a useful tool to study phenomena in the experiments of Gawlitta *et al.*[10]

Hypoxia was assumed to decrease tissue viability and hence increase the medium LDH concentration, through its effect on glucose consumption. Oxygen shortage necessitates the cells to shift to anaerobic metabolism, resulting in lactate as the final breakdown product of glucose consumption. Indeed, to obtain a good fit to the experimental data (Fig. 5), the ratio between lactate production and glucose consumption had to be increased with respect to the control experiment. Moreover, the negative feedback of lactate on glucose consumption had to be decreased, allowing more glucose consumption at relatively high lactate concentrations.

It is interesting to note that these effects of hypoxia were not visible when hypoxia was induced in combination with lactic acidification. In that case, no parameter adaptation was needed to fit the experimental results because there were hardly any differences between the lactic acidification experiments in the presence or absence of hypoxia (Fig. 7). The observed decrease in glucose metabolism associated with lactic acidification might reduce the need for oxygen and hence make the tissue less sensitive to hypoxia.

Pure lactic acidification decreased glucose consumption through lactate accumulation. This, in turn, led to increases in LDH concentrations with decreasing pH. In the experiments from Gawlitta *et al.*,[10] no differences were observed in LDH concentrations for the experiments with pH values of 6.5 and 6.0 compared to the control experiment with pH 7.4. Only a pH of 5.3 significantly increased experimental LDH values (Fig. 4). An explanation for this difference between the experiments and the numerical predictions could be that the effect of lactate on LDH release is nonlinear, opposed to the linear effect that was assumed in the model. However, the experimental LDH concentrations disagreed with the results from the MTT assays at day 5, an alternative indication of viability. MTT absorption reflects metabolic activity of the tissue, and decreases when cell death increases or cell metabolism decreases. LDH leaks out of cells when the integrity of their membranes has been compromised, and increases when viability decreases. Gawlitta *et al.*[10] found a monotonic decrease in MTT absorption for decreasing pH values, which corresponded well to the numerically predicted LDH values.

In compression experiments, LDH concentrations and MTT assays also disagreed. Indeed, MTT data showed a significant decrease in viability due to deformation whereas no effect was observed in LDH concentrations. Accordingly, no effect of deformation on LDH leakage was initially included in the model. However, earlier experiments by Gawlitta *et al.*,[9] Wang *et al.*,[20] and Breuls *et al.*[4] did demonstrate a reduction in viability when tissue-engineered constructs were subjected to compression. This disagreement could be due to the limited diffusion of LDH.[10]

Indeed, Gefen *et al.*[11] recently demonstrated a 50% reduction in the diffusion coefficient of molecules the size of LDH as a result of compression of the same tissue-engineered muscle constructs as were used by Gawlitta *et al.*[10] Combined with the change in geometry due to the weight that was imposed on the construct, this diffusion limitation led to an accumulation of LDH inside the constructs. This led to a discrepancy between the observed and predicted LDH concentrations for deformation experiments, which could be accommodated by increasing the cell death rate on day 1 to account for the short-term harmful effect of deformation (Figs. 6 and 8).

When deformation was combined with hypoxia, the same increase in cell death rate during day 1 could explain the observed LDH concentrations. Damage was the sum of damage due to deformation and hypoxia, and no interaction between the two damage mechanisms had to be included in the model to predict the measured LDH concentrations. This suggests that at least in the tissue-engineered muscle constructs,

there is no synergistic effect of deformation and hypoxia.

Another effect of compression was a slight over-estimation of the glucose concentrations and under-estimation of the lactate concentrations (Fig. 5). The weight on top of the construct limited diffusion of these metabolites to and from the medium. This effect might be slightly over-estimated since the model assumed that the complete construct was compressed whereas the weight did not cover the extremities of the constructs in the experiments.

In conclusion, the most important finding of the present study was that deformation did cause LDH leakage although no effect was observed on LDH concentrations in the medium.[10] Thus, the measured LDH concentrations during compression did not reflect the true LDH leakage in the construct.

The kind of experiment that Gawlitta et al.[10] performed is quite common in tissue-engineering labora-tories, i.e., the effects of all kinds of stimuli are assessed through measurement of biochemical markers in medium. The current paper shows that a proper description of transport processes that are involved is essential for a correct interpretation of the results of such experiments.

APPENDIX

A finite element code was written to solve the set of Eqs. in (1)–(3). A list of symbols is included in Table 4.

TABLE 4. List of symbols.

C_{GL}	Glucose concentration
C_{LA}	Lactate concentration
C_{LDH}	LDH concentration
$\bar{C}_{LDH}$	Average LDH concentration in medium and construct
D_{GL}	Glucose diffusion coefficient
D_{LA}	Lactate diffusion coefficient
D_{LDH}	LDH diffusion coefficient
Γ	Boundary of domain Ω
GL	Glucose
ℓ_1	Basal cell death rate
ℓ_2	Parameter defining LDH increase when glucose availability is too low
ℓ_3	Threshold value for glucose availability
ℓ_4	Parameter defining LDH increase when lactate concentration is too high
ℓ_5	Threshold value for lactate concentration
ℓ_6	Average LDH concentration when all cells are dead
f_{LA}	Parameter defining inhibiting effect of LA on GL consumption
$f_{\frac{LA}{GL}}$	Ratio between LA production and GL consumption
K_m	Glucose concentration at half maximum consumption rate
LA	Lactate
LDH	Lactate dehydrogenase
V_m	Maximum glucose consumption rate

First, the weak forms are obtained by multiplication of Eqs. (1)–(3) by a weighting function (v), integration over Ω, followed by integration by parts to remove the second derivative in the diffusion term:

$$\int_\Omega v \frac{\partial C_{GL}}{\partial t} d\Omega$$
$$- \int_\Gamma v\vec{n} D_{GL} \vec{\nabla} C_{GL} d\Gamma + \int_\Omega D_{GL} \vec{\nabla} v (\vec{\nabla} C_{GL}) d\Omega$$
$$+ \int_\Omega v(\ell_6 - \bar{C}_{LDH})(1 - f_{LA} C_{LA}) \frac{V_m C_{GL}}{K_m + C_{GL}} d\Omega = 0$$

(4)

$$\int_\Omega v \frac{\partial C_{LA}}{\partial t} d\Omega$$
$$- \int_\Gamma v\vec{n} D_{LA} \vec{\nabla} C_{LA} d\Gamma + \int_\Omega D_{LA} \vec{\nabla} v (\vec{\nabla} C_{LA}) d\Omega$$
$$+ \int_\Omega v f_{\frac{LA}{GL}}(\ell_6 - \bar{C}_{LDH})(1 - f_{LA} C_{LA}) \frac{V_m C_{GL}}{K_m + C_{GL}} d\Omega = 0$$

(5)

$$\int_\Omega v \frac{\partial C_{LDH}}{\partial t} d\Omega$$
$$- \int_\Gamma v\vec{n} D_{LDH} \vec{\nabla} C_{LDH} d\Gamma + \int_\Omega D_{LDH} \vec{\nabla} v (\vec{\nabla} C_{LDH}) d\Omega$$
$$- \int_\Omega v \left(\ell_1 + \ell_2 \left(\ell_3 - \frac{\partial C_{GL}}{\partial t} \right) + \ell_4 (C_{LA} + \ell_5) \right) d\Omega = 0$$

(6)

The nonlinear Michaelis–Menten term requires line-arization, i.e., substituting $f(C) = f(\hat{C}) + \delta f(\hat{C})$, in which f is an arbitrary function of C and $\hat{C}$ is an estimation of C. Here, $\hat{C}$ will simply be called C. The result is the following linearized set of equations:

$$\int_\Omega v \frac{\partial C_{GL}}{\partial t} d\Omega + \int_\Omega v \frac{\partial \delta C_{GL}}{\partial t} d\Omega$$
$$+ \int_\Omega D_{GL} \vec{\nabla} v (\vec{\nabla} C_{GL}) d\Omega + \int_\Omega D_{GL} \vec{\nabla} v (\vec{\nabla} \delta C_{GL}) d\Omega$$
$$+ \int_\Omega v(\ell_6 - \bar{C}_{LDH})(1 - f_{LA} C_{LA}) \frac{V_m C_{GL}}{K_m + C_{GL}} d\Omega$$
$$+ \int_\Omega v(\ell_6 - \bar{C}_{LDH})(1 - f_{LA} C_{LA}) \frac{V_m K_m}{(K_m + C_{GL})^2} \delta C_{GL} d\Omega$$
$$- \int_\Omega v(\ell_6 - \bar{C}_{LDH}) \frac{V_m C_{GL}}{K_m + C_{GL}} f_{LA} \delta C_{LA} d\Omega = 0 \quad (7)$$

$$\int_\Omega v\frac{\partial C_{LA}}{\partial t}d\Omega + \int_\Omega v\frac{\partial \delta C_{LA}}{\partial t}d\Omega$$

$$+ \int_\Omega D_{LA}\vec\nabla v(\vec\nabla C_{LA})d\Omega + \int_\Omega D_{LA}\vec\nabla v(\vec\nabla \delta C_{LA})d\Omega$$

$$+ \int_\Omega vf_{\frac{LA}{GL}}(\ell_6 - \bar C_{LDH})(1 - f_{LA}C_{LA})\frac{V_m C_{GL}}{K_m + C_{GL}}d\Omega$$

$$+ \int_\Omega vf_{\frac{LA}{GL}}(\ell_6 - \bar C_{LDH})(1 - f_{LA}C_{LA})\frac{V_m K_m}{(K_m + C_{GL})^2}\delta C_{GL}d\Omega$$

$$- \int_\Omega vf_{\frac{LA}{GL}}(\ell_6 - \bar C_{LDH})\frac{V_m C_{GL}}{K_m + C_{GL}}f_{LA}\delta C_{LA}d\Omega = 0 \qquad (8)$$

$$\int_\Omega v\frac{\partial C_{LDH}}{\partial t}d\Omega + \int_\Omega v\frac{\partial \delta C_{LDH}}{\partial t}d\Omega$$

$$+ \int_\Omega D_{LDH}\vec\nabla v(\vec\nabla C_{LDH})d\Omega + \int_\Omega D_{LDH}\vec\nabla v(\vec\nabla \delta C_{LDH})d\Omega$$

$$- \int_\Omega v\left(\ell_1 + \ell_2\left(\ell_3 - \frac{\partial C_{GL}}{\partial t}\right) + \ell_4(C_{LA} + \ell_5)\right)d\Omega$$

$$- \int_\Omega v\left(-\ell_2\frac{\partial \delta C_{GL}}{\partial t} + \ell_4\delta C_{LA}\right)d\Omega = 0 \qquad (9)$$

After linearization, spatial discretization was performed through application of the Galerkin method to find polynomial approximations of solutions for C in each element $e(\underset{\sim}{N}^T\underset{\sim e}{C})$. $\underset{\sim}{N}$ is a set of shape functions that is both applied to the solute concentrations and to the weighting function v. After some rearrangements, $\underset{\sim e}{v}$ cancels out and summation over all elements leads to the following set of equations:

$$\underline{M}\frac{\partial \delta \underset{\sim}{C}_{GL}}{\partial t} + D_{GL}\underline{K}\delta\underset{\sim}{C}_{GL} + (1 - f_{LA}LA)\underline{MM}\delta\underset{\sim}{C}_{GL}$$

$$- f_{LA}\underline{MMc}\delta\underset{\sim}{C}_{LA} = -\underline{M}\frac{\partial \underset{\sim}{C}_{GL}}{\partial t}$$

$$- D_{GL}\underline{K}\underset{\sim}{C}_{GL} - (1 - f_{LA}LA)\underline{MMr}\delta\underset{\sim}{C}_{GL} \qquad (10)$$

$$\underline{M}\frac{\partial \delta \underset{\sim}{C}_{LA}}{\partial t} + D_{LA}\underline{K}\delta\underset{\sim}{C}_{LA} + f_{\frac{LA}{GL}}(1 - f_{LA}LA)\underline{MM}\delta\underset{\sim}{C}_{GL}$$

$$- f_{\frac{LA}{GL}}f_{LA}\underline{MMc}\delta\underset{\sim}{C}_{LA} = -\underline{M}\frac{\partial \underset{\sim}{C}_{LA}}{\partial t}$$

$$- D_{LA}\underline{K}\underset{\sim}{C}_{LA} - f_{\frac{LA}{GL}}(1 - f_{LA}LA)\underline{MMr}\underset{\sim}{C}_{GL} \qquad (11)$$

$$\underline{M}\frac{\partial \delta \underset{\sim}{C}_{LDH}}{\partial t} + D_{LDH}\underline{K}\delta\underset{\sim}{C}_{LDH} + \ell_2\underline{M}\frac{\partial \delta \underset{\sim}{C}_{GL}}{\partial t}$$

$$- \ell_4\underline{M}\delta\underset{\sim}{C}_{LA} = -\underline{M}\frac{\partial \underset{\sim}{C}_{LDH}}{\partial t}$$

$$- D_{LDH}\underline{K}\underset{\sim}{C}_{LDH} - \ell_2\underline{M}\frac{\partial \underset{\sim}{C}_{GL}}{\partial t} + \ell_4\underline{M}\underset{\sim}{C}_{LA} + \underset{\sim}{L} \qquad (12)$$

with the following definitions:

$$\underline{M} = \int_\Omega \underset{\sim}{N}\underset{\sim}{N}^T d\Omega$$

$$\underline{K} = \int_\Omega \underset{\sim}{\nabla N}(\underset{\sim}{\nabla N}^T)d\Omega$$

$$LA = \underset{\sim}{N}^T\underset{\sim}{C}_{LA}$$

$$\underline{MM} = (\ell_6 - \bar C_{LDH})\int_\Omega \underset{\sim}{N}\frac{V_m K_m}{(K_m + \underset{\sim}{N}^T\underset{\sim}{C}_{GL})^2}\underset{\sim}{N}^T d\Omega$$

$$\underline{MMc} = (\ell_6 - \bar C_{LDH})\int_\Omega \underset{\sim}{N}\frac{V_m \underset{\sim}{N}^T\underset{\sim}{C}_{GL}}{K_m + \underset{\sim}{N}^T\underset{\sim}{C}_{GL}}\underset{\sim}{N}^T d\Omega$$

$$\underline{MMr} = (\ell_6 - \bar C_{LDH})\int_\Omega \underset{\sim}{N}\frac{V_m K_m}{(K_m + \underset{\sim}{N}^T\underset{\sim}{C}_{GL})^2}\underset{\sim}{N}^T d\Omega$$

$$\underset{\sim}{L} = \int_\Omega \underset{\sim}{N}(\ell_1 + \ell_2\ell_3 + \ell_4\ell_5)d\Omega \qquad (13)$$

Temporal discretization was subsequently applied through the θ-scheme:

$$\underline{M}\frac{\delta \underset{\sim}{C}_{GL}^{n+1} - \delta \underset{\sim}{C}_{GL}^n}{\Delta t} + \theta D_{GL}\underline{K}\delta\underset{\sim}{C}_{GL}^{n+1}$$

$$+ (1-\theta)D_{GL}\underline{K}\delta\underset{\sim}{C}_{GL}^n + \theta(1 - f_{LA}LA)\underline{MM}\delta\underset{\sim}{C}_{GL}^{n+1}$$

$$+ (1-\theta)(1 - f_{LA}LA)\underline{MM}\delta\underset{\sim}{C}_{GL}^n - \theta f_{LA}\underline{MMc}\delta\underset{\sim}{C}_{LA}^{n+1}$$

$$- (1-\theta)f_{LA}\underline{MMc}\delta\underset{\sim}{C}_{LA}^n = -\underline{M}\frac{\underset{\sim}{C}_{GL}^{n+1} - \underset{\sim}{C}_{GL}^n}{\Delta t}$$

$$- \theta D_{GL}\underline{K}\underset{\sim}{C}_{GL}^{n+1} - (1-\theta)D_{GL}\underline{K}\underset{\sim}{C}_{GL}^n$$

$$- \theta(1 - f_{LA}LA)\underline{MMr}\underset{\sim}{C}_{GL}^{n+1}$$

$$- (1-\theta)(1 - f_{LA}LA)\underline{MMr}\underset{\sim}{C}_{GL}^n \qquad (14)$$

$$\underline{M}\frac{\delta \underset{\sim}{C}_{LA}^{n+1} - \delta \underset{\sim}{C}_{LA}^n}{\Delta t} + \theta D_{LA}\underline{K}\delta\underset{\sim}{C}_{LA}^{n+1}$$

$$+ (1-\theta)D_{LA}\underline{K}\delta\underset{\sim}{C}_{LA}^n + \theta f_{\frac{LA}{GL}}(1 - f_{LA}LA)\underline{MM}\delta\underset{\sim}{C}_{GL}^{n+1}$$

$$+ (1-\theta)f_{\frac{LA}{GL}}(1 - f_{LA}LA)\underline{MM}\delta\underset{\sim}{C}_{GL}^n$$

$$- \theta f_{\frac{LA}{GL}}f_{LA}\underline{MMc}\delta\underset{\sim}{C}_{LA}^{n+1} - (1-\theta)f_{\frac{LA}{GL}}f_{LA}\underline{MMc}\delta\underset{\sim}{C}_{LA}^n$$

$$= -\underline{M}\frac{\underset{\sim}{C}_{LA}^{n+1} - \underset{\sim}{C}_{LA}^n}{\Delta t} - \theta D_{LA}\underline{K}\underset{\sim}{C}_{LA}^{n+1} - (1-\theta)D_{LA}\underline{K}\underset{\sim}{C}_{LA}^n$$

$$- \theta f_{\frac{LA}{GL}}(1 - f_{LA}LA)\underline{MMr}\underset{\sim}{C}_{GL}^{n+1}$$

$$- (1-\theta)f_{\frac{LA}{GL}}(1 - f_{LA}LA)\underline{MMr}\underset{\sim}{C}_{GL}^n \qquad (15)$$

$$
\underline{M}\frac{\delta C^{n+1}_{\sim \text{LDH}} - \delta C^n_{\sim \text{LDH}}}{\Delta t} + \theta D_{\text{LDH}}\underline{K}\delta C^{n+1}_{\sim \text{LDH}}
$$

$$
+ (1-\theta)D_{\text{LDH}}\underline{K}\delta C^n_{\sim \text{LDH}} + \ell_2 \underline{M}\frac{\delta C^{n+1}_{\sim \text{GL}} - \delta C^n_{\sim \text{GL}}}{\Delta t}
$$

$$
- \theta \ell_4 \underline{M}\delta C^{n+1}_{\sim \text{LA}} - (1-\theta)\ell_4 \underline{M}\delta C^n_{\sim \text{LA}}
$$

$$
= -\underline{M}\frac{C^{n+1}_{\sim \text{LDH}} - C^n_{\sim \text{LDH}}}{\Delta t} - \theta D_{\text{LDH}}\underline{K}C^{n+1}_{\sim \text{LDH}}
$$

$$
- (1-\theta)D_{\text{LDH}}\underline{K}C^n_{\sim \text{LDH}} - \ell_2 \underline{M}\frac{C^{n+1}_{\sim \text{GL}} - C^n_{\sim \text{GL}}}{\Delta t}
$$

$$
+ \theta \ell_4 \underline{M}C^{n+1}_{\sim \text{LA}} + (1-\theta)\ell_4 \underline{M}C^n_{\sim \text{LA}} + \underline{L}_{\sim} \tag{16}
$$

In the above equations $C^n_{\sim}$ is the converged concentration in the previous time increment, $\delta C^n_{\sim}$ is the iterative concentration change in the previous increment, which approximates zero by definition, and hence, all terms containing this expression can be neglected. $C^{n+1}_{\sim}$ is the last updated concentration in the current time increment, and $\delta C^{n+1}_{\sim}$ is the concentration change to be calculated.

That leads to the following arrays that were implemented in Matlab:

REFERENCES

[1]Allhands, R. V., P. A. Torzilli, and F. A. Kallfelz. Measurement of diffusion of uncharged molecules in articular cartilage. *Cornell Vet.* 74:111–123, 1983.

[2]Blaisdell, F. W. The pathophysiology of skeletal muscle ischemia and the reperfusion symdrome: a review. *Cardiovasc. Surg.* 10(6):620–630, 2002.

[3]Bouten, C. V. C., M. M. Knight, D. A. Lee, and D. L. Bader. Compressive deformation and damage of muscle cell subpopulations in a model system. *Ann. Biomed. Eng.* 29:153–163, 2001.

[4]Breuls, R. G. M., C. V. C. Bouten, C. W. J. Oomens, D. L. Bader, and F. P. T. Baaijens. Compression induced cell damage in engineered muscle tissue: an *in vitro* model to study pressure ulcer aetiology. *Ann. Biomed. Eng.* 31:1357–1364, 2003.

[5]Cabrera, M. E., G. M. Saidel, and S. C. Kalhan. Role of O₂ in regulation of lactate dynamics during hypoxia: mathemaitcal model and analysis. *Ann. Biomed. Eng.* 26:1–27, 1998.

[6]Cox, M. A. J., D. Gawlitta, N. J. B. Driessen, C. W. J. Oomens, and F. P. T. Baaijens. Non-linear mechanical properties of soft engineered biological tissues determined by finite spherical indentation. *Comput. Methods Biomech. Biomed. Eng.* 2007. doi:10.1080/10255840701771768.

[7]Daniel, R. K., D. L. Priest, and D. C. Wheatley. Etiologic factors in pressure sores: an experimental model. *Arch. Phys. Med. Rehabil.* 62:492–498, 1981.

[8]Dash, R. K., J. A. DiBella, and M. E. Cabrera. A computational model of skeletal muscle metabolism linking

$$
\begin{bmatrix}
\underline{M}\frac{1}{\Delta t} + \theta(D_{\text{GL}}\underline{K} + (1-f_{\text{LA}}\text{LA})\underline{MM}) & -\theta f_{\text{LA}}\underline{MM}c & \underline{0} \\
\theta f_{\frac{\text{LA}}{\text{GL}}}(1-f_{\text{LA}}\text{LA})\underline{MM} & \underline{M}\frac{1}{\Delta t} + \theta(D_{\text{LA}}\underline{K} - f_{\frac{\text{LA}}{\text{GL}}}f_{\text{LA}}\underline{MM}c) & \underline{0} \\
\ell_2\underline{M}\frac{1}{\Delta t} & -\theta\ell_4\underline{M} & \underline{M}\frac{1}{\Delta t} + \theta D_{\text{LDH}}\underline{K}
\end{bmatrix}
\begin{bmatrix}
\partial C_{\sim \text{GL}} \\
\partial C_{\sim \text{LA}} \\
\partial C_{\sim \text{LDH}}
\end{bmatrix}_{n+1}
=
$$

$$
\begin{bmatrix}
-\underline{M}\frac{1}{\Delta t} - \theta(D_{\text{GL}}\underline{K} + (1-f_{\text{LA}}\text{LA})\underline{MM}r) & \underline{0} & \underline{0} \\
-\theta f_{\frac{\text{LA}}{\text{GL}}}(1-f_{\text{LA}}\text{LA})\underline{MM}r & -\underline{M}\frac{1}{\Delta t} - \theta D_{\text{LA}}\underline{K} & \underline{0} \\
-\ell_2\underline{M}\frac{1}{\Delta t} & +\theta\ell_4\underline{M} & -\underline{M}\frac{1}{\Delta t} - \theta D_{\text{LDH}}\underline{K}
\end{bmatrix}_{n+1}
\begin{bmatrix}
C_{\sim \text{GL}} \\
C_{\sim \text{LA}} \\
C_{\sim \text{LDH}}
\end{bmatrix}_{n+1}
$$

$$
+
\begin{bmatrix}
\underline{M}\frac{1}{\Delta t} - (1-\theta)(D_{\text{GL}}\underline{K} + (1-f_{\text{LA}}\text{LA})\underline{MM}r) & \underline{0} & \underline{0} \\
-(1-\theta)f_{\frac{\text{LA}}{\text{GL}}}(1-f_{\text{LA}}\text{LA})\underline{MM}r & \underline{M}\frac{1}{\Delta t} - (1-\theta)D_{\text{LA}}\underline{K} & \underline{0} \\
\ell_2\underline{M}\frac{1}{\Delta t} & (1-\theta)\ell_4\underline{M} & \underline{M}\frac{1}{\Delta t} - (1-\theta)D_{\text{LDH}}\underline{K}
\end{bmatrix}_n
\begin{bmatrix}
C_{\sim \text{GL}} \\
C_{\sim \text{LA}} \\
C_{\sim \text{LDH}}
\end{bmatrix}_n
+
\begin{bmatrix}
0_{\sim} \\
0_{\sim} \\
L_{\sim}
\end{bmatrix}
\tag{17}
$$

cellular adaptations induced by altered loading states to metabolic responses during exercise. *Biomed. Eng.* 2007. doi:10.1186/1475-925X-6-14.

[9]Gawlitta, D., W. Li, C. W. J. Oomens, F. P. T. Baaijens, D. L. Bader, and C. V. C. Bouten. The relative contributions of compression and hypoxia to development of muscle tissue damage: an *in vitro* study. *Ann. Biomed. Eng.* 35(2):273–284, 2007.

[10]Gawlitta, D., C. W. J. Oomens, D. L. Bader, F. P. T. Baaijens, and C. V. C. Bouten. Temporal differences in the influence of ischemic factors and deformation on the metabolism of engineered skeletal muscle. *J. Appl. Physiol.* 103(2):464–473, 2007.

[11]Gefen, A., L. H. Cornelissen, D. Gawlitta, D. Bader, and C. W. J. Oomens. The free diffusion of macromolecules in tissue-engineered skeletal muscle subjected to large compression strains. *J. Biomech.* 2007. doi:10.1016/j.jbiomech.2007.10.023.

[12]Grisotto, P. C., A. C. Santos dos, J. Coutinho-Netto, J. Cherri, and C. E. Piccinato. Indicators of oxidative injury and alterations of the cell membrane in the skeletal muscle of rats submitted to ischemia and reperfusion. *J. Surg. Res.* 92:1–6, 2000.

[13]Holm, S., A. Maroudas, J. P. G. Urban, G. Selstam, and A. Nachemson. Nutrition of the intervertebral disc: solute transport and metabolism. *Connect. Tissue Res.* 8:101–119, 1981.

[14]Korzeniewski, B., and P. Liguzinski. Theoretical studies on the regulation of anaerobic glycolysis and its influence on oxidative phosphorylation in skeletal muscle. *Biophys. Chem.* 110:147–169, 2004.

[15]Kosiak, M. Etiology and pathology of ischemic ulcers. *Arch. Phys. Med. Rehabil.* 40:62–69, 1959.

[16]Lambeth, M. J., and M. J. Kushmerick. A computational model for glycogenolysis in skeletal muscle. *Ann. Biomed. Eng.* 30:808–827, 2002.

[17]Maroudas, A. Biophysical chemistry of cartilaginous tissues with special reference to solute and fluid transport. *Biorheology* 12:233–248, 1975.

[18]Reddy, N. P., and K. Patel. A mathematical model of flow through the terminal lymphatics. *Med. Eng. Phys.* 17(2):134–140, 1995.

[19]Stekelenburg, A., G. J. Strijkers, H. Parusel, D. L. Bader, K. Nicolay, and C. W. J. Oomens. The role of ischemia and deformation in the onset of compression-induced deep tissue injury: MRI-based studies in a rat model. *J. Appl. Physiol.* 102(5):2002–2011, 2007.

[20]Wang, Y.-N., C. V. C. Bouten, D. A. Lee, and D. L. Bader. Compression-induced damage in a muscle cell model *in vitro*. *P. I. Mech. Eng. H.* 219(1):1–12, 2005.